Proceedings of the ASME/BATH
Symposium on Fluid Power and Motion Control
FPMC2021
October 19-21, 2021, Virtual Conference, Online

FPMC2021-68484

PIPELINE MODEL FIDELITY FOR WAVE ENERGY SYSTEM MODELS

Jeremy W. Simmons II
Department of Mechanical Engineering
University of Minnesota
Minneapolis, MN, USA
simmo536@umn.edu

James D. Van de Ven
Department of Mechanical Engineering
University of Minnesota
Minneapolis, MN, USA
vandeven@umn.edu

ABSTRACT

Ocean wave energy conversion plants that use hydraulic power take-offs (PTOs) have been configured so that the working fluid must travel a significant distance (of several hundred to a few thousand meters) from the wave energy converter (WEC) located offshore to equipment onshore. With the pulsatile flow generated by the WEC having a peak period in the range of 3 to 12 seconds, the wavelengths of the excited pressure waves approach the length of the pipelines themselves. By the standards for modeling pipelines presented in popular fluid power and related textbooks, the system models for these plants should include distributed parameter models of the pipeline dynamics that capture the pressure wave delay effects. This work tests the importance of pipeline model fidelity for wave energy conversion plants. Simulations have been conducted of a simple but representative hydraulic PTO for wave energy conversion and incorporate several common lumped and distributed parameter pipeline models for comparison. These results are used to show the degree to which model fidelity effects several design metrics that are especially useful in the preliminary design phase of system development. The pipeline models used include: 1) a short line model that includes lumped resistive effects only, 2) a medium line model that also includes lumped inertial and capacitive effects for a single pipeline segment, 3) a long line model that uses repeated, lumped parameter line segments to approximate the distributed parameters of a real pipeline, 4) a simple method of characteristics solution to the one-dimensional momentum and continuity equations assuming a fixed wave speed, and 5) a discrete free-gas cavity model augmenting the simple method of characteristic pipeline model. The results suggest a relaxed standard for modeling pipelines in the case of this type of system, in which case, the recommended model is easily implemented in variable time step solvers and CAD software such as Simscape Fluids and can be used within the WEC-Sim modeling framework developed by the National Renewable Energy Lab.

INTRODUCTION

Ocean wave-powered, reverse osmosis (RO) systems with hydraulic power take-offs (PTOs), like conventional desalination plants, are likely to included long pipelines. However, prior published work has not considered the effects that pipelines may have on the dynamics of wave energy PTOs. In this work we present a study comparing pipeline modeling techniques in the context of a generic, hydraulic PTO in normal operation. The study is conducted to 1) reveal the significance of various attributes of long pipelines and 2) recommend pipeline modeling techniques for use in system models that are built to estimate metrics like power loss and variation in pressure under normal operation of the plant.

Background

The global resource for power in wind-generated ocean waves has been estimated to be about 2.1 TW [1], which is the equivalent of about 12 percent of the world average power consumption in 2018 of 18 TW [2,3]. Coastal regions with convenient access to wave resources could benefit from conversion of this power to either electricity or the production of fresh water using wave-powered desalination processes. Researchers found wave-powered RO to be feasible for the arid Gran Canaria Island [4] and to be reasonably cost competitive in the drought prone state of California [5].

As a way to reduce cost and improve the efficiency of a wave-powered desalination process, a community of researchers and a developing wave energy industry have considered integrating the reverse osmosis process into a hydraulic circuit to make up the wave energy converter's (WEC) PTO [6–10]. RO desalination is a membrane-based process used to separate water from dissolved solids using fluid pressure as a driving force for the separation; a WEC-driven pump serves to pressurize seawater to be desalinated. Integrating the hydraulic circuits of the RO process and PTO, rather than producing electricity that then drives a

conventional RO system, avoids at least three stages of power conversion (mechanical power to electrical power, then back to mechanical power and on to hydraulic power).

The wave energy conversion process is a characteristically variable process, whereas conventional RO processes are characteristically steady. Some constraints on the dynamic behavior of the PTO must be considered to avoid damage to RO system components that are conventionally designed for steady operation. Membrane manufactures specify a variety of constraints that would limit the dynamic fluctuation of an RO system such as a limited range of operating pressure (e.g. 4-7 MPa) and a maximum rate of change in pressure (70 kPa per second) [11–13]. Other constraints may develop as the design of these system matures and failure mechanisms of RO components are better understood, such as fatigue limits on the RO membrane which has yet to be characterized [14].

Although prior modeling and design analyses given in the literature may be adequate for initial estimates of performance, the model fidelity may be inadequate for performing effective design without accounting for pipeline dynamics. In fact, no published work on wave energy converters has considered the presence of long pipelines despite these being a likely feature. This includes both wave-powered RO [9,15] and electrical power producing systems [16] that have a hydraulic PTO.

To illustrate the scale of pipelines and their excitations in wave-energy systems, consider the electric power producing prototype plant built by Aquamarine Power, called Oyster 1 [16]. This WEC was placed 500 meters offshore while its turbine and electric generator were placed onshore. These two parts of the plant were connected by 500-meter-long, high-pressure and low-pressure pipelines. Depending on the geography of the seabed, the pipeline may be anywhere between 300 and 1500 meters long [15]. In addition, the pulsations generated by the WEC-driven pumps would typically falling in the range of three to ten seconds (half the peak wave period which is typically between 6 and 20 seconds). For these conditions, the wavelengths of the pressure waves traveling in the working fluid approach the same order of distance as the length of the pipeline (considering wave speeds between 800 and 1500 meters per second). At this scale, the pipeline dynamics may have important effects on plant performance and on the pressure variation at the RO module. Therefore, it is important to know what models of pressure and flow though pipelines are adequate for effective system design.

Pipeline Classification, Modeling Techniques, and Guidelines

The spectrum of pipeline modeling techniques includes a variety of lumped parameter and distributed parameter methods. Lumped parameter methods lump the resistive, inertive, and capacitive effects of the pipeline into discrete elements arranged as shown in Figure 1 for short, medium, and long lines (pipelines). Resistance is often described by the Darcy-Weisbach equation while the inertia and capacitance effects are described by the relevant ordinary differential equations (ODEs). Distributed parameter models account for the wave delay explicitly and are either direct solutions or approximation of to the partial differential equations (PDEs) for one-dimensional flow.

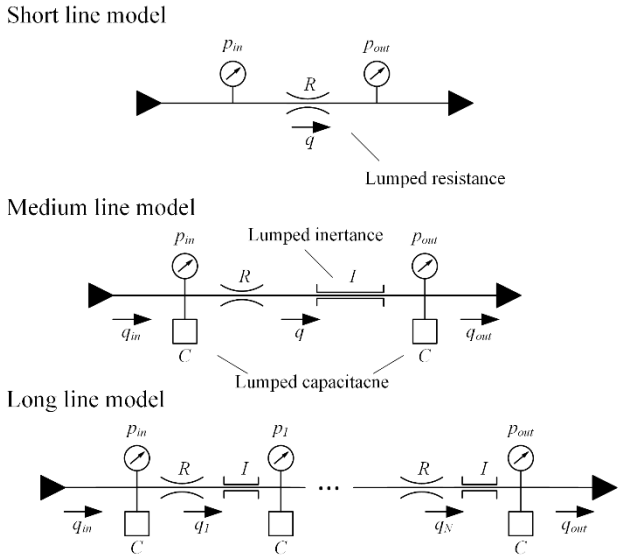

FIGURE 1. LUMPED PARAMETER PIPELINE MODEL CONFIGURATIONS HAVING RESISTIVE (R), CAPACITIVE (C), AND INERTIVE (I) PROPERTIES: (TOP) SHORT LINE, (MIDDLE) MEDIUM LINE, AND (BOTTOM) THE LONG LINE, N π-LUMP MODEL

As suggested by Figure 1, lumped parameter models are classified by the length of pipe they can model. Short lines are adequately described by their flow resistance, while the effects of medium lines are better characterized by a configuration of lumped capacitive, resistive, and inertive elements as shown for the medium line model in Figure 1. This configuration of elements for the medium line model has been referred to the nominal π [17] and is referred to as a π-lump here. Long lines are best described by distributed parameter models with the continuously distributed nature of the resistance, capacitance, and inertance accounting for the finite speed of pressure waves: however, an approach to approximating the distributed nature of the pipeline is to model the pipeline as a series of N π-lumps as shown in Figure 1 for the long line model [18].

Distributed parameter methods are diverse and a subject of study for many researchers [19], including comparative studies that focus on efficiency and accuracy [20,21]. The most familiar methods to the wider engineering community might be the numerical approaches of finite-difference and finite-volume methods. Some advanced one-dimensional, finite-volume, Godunov-type schemes offer a high degree of efficiency, accuracy, and flexibility [22,23]. Other methods like modal approximation [20] and the transmission line model [24,25] are efficient and have been subject to developments aimed at

improving accuracy and robustness. However, these are restricted to linear, constant parameter cases.

Methods using the method of characteristics (MOC) have been well regarded for their accuracy, efficiency, and ease of implementation [19,26]. These have also been modified and used to capture a high degree of nonlinearity, including cavitation and column separation [27,28]. Using the MOC, the system of PDEs describing one-dimensional flow in a pipeline are reduced to a system of ODEs valid along positive and negative characteristics. In many implementations, the system of ODEs is integrated analytically along the characteristics to give an explicit system of equations for the next time step of a simulation. The drawback of this method is that it is restricted to a fixed time step solution, requiring methods like interpolation to couple the model to variable time step solvers and to model pipe networks that include pipelines of variable length.

The most common implementation of the MOC-based pipeline models assumes a fixed speed of sound and neglects the effect of the fluid velocity on the wave speed. The MOC method can also be augmented with the discrete gas cavity model (DGCM) to account for the effects of entrained air on the speed of sound in the fluid and can be used to capture cavitation in the pipeline [27,28].

There are several guidelines provided in literature to guide the selection of pipeline models (i.e. lumped versus distributed parameter). Wylie and Streeter [28] recommend distributed parameter models for all transient problems but conceded that when computational cost is a concern, lumped parameter models (short and medium lines) may be adequate for pipelines whose lengths are less than 4 percent of the wavelength of pipeline excitations. That is where the wavelength (L_w) is determined from speed of sound in the fluid (a) and the frequency of the excitation (f_e) such that

$$L_w = \frac{a}{f_e} \quad (1).$$

For the analysis of electrical power lines, which are analogous to fluid filled pipelines, Grainger and Stevenson [17] also recommend a classification based on line lengths such that short line models are used for lines shorter than $0.016L_w$ and medium line models are used for longer lines, up to $0.046L_w$; otherwise the lumped, long line model or distributed parameter models should be used. Finally, Watton [18] recommends an order-of-magnitude comparison of time constants within the problem under consideration.

The context of recommendations for modeling practice should be considered. Early work on pipeline transient, on which [28] was largely based, was focused on analysis of water hammer events arising from transients inducing events like sudden valve closures and pump start-up, possibly in piping networks. The analysis in [17] is focused on electrical power systems that operated nominally under highly regular alternating current, may be disturbed by similarly strong transients, and must meet constraints placed on electrical infrastructure. Watton [18] is concerned with conventional fluid power problems, much of which is oriented towards feedback control of the system [20] (for which modal analysis is the favored approach). The strength of transients in each case are different and analysis is oriented toward different concerns and design methods.

The context of wave energy is different in several ways from those in which the guidelines above originate, suggesting that different guidelines might be more appropriate. Yet, these differences are in contradiction with each other and it is not clear how these guidelines should be treated for wave energy systems. 1) Waves forcing the system are best characterized by a continuous distribution of frequency components spanning about two orders of magnitude rather than simple sinusoidal signals or by step and ramp inputs (see Figure 2 for an example of a power spectral density function used to describe realistic wave elevations and a constructed timeseries for wave elevation at a single location over time). This wide range in excitation frequency suggests that the peak frequency of the waves might not suffice for evaluating the length of the pipeline. 2) The degree to which power smoothing is necessary for these systems would result weaker transients compared to transients like those excited by sudden valve closure. Design metrics might be captured well enough by lower fidelity models where transients are relatively weak, even if the exciting frequency is within that range of pipelines natural frequency. 3) Finally, the fragility of a conventional RO membrane elements and the extreme constraints which manufactures place on their use suggests that even weak transients may be important, and that higher model accuracy is needed.

With these contradicting observations, it is not clear whether the modeling guidelines found in the literature are applicable to the analysis of hydraulic PTO designs considered for wave energy applications. Therefore, this work compares results of the relevant modeling techniques in the context of a simple, but representative, hydraulic PTO circuit. Several metrics are considered that have the potential to highlight the effects of pressure variation and wave delay. The following section describes the methods used in this study and is followed by the formulation of the mathematical models used, along with their implementation. Then the results are presented which are followed by a discussion and conclusions from the study.

METHODS

This study considers the performance of five different pipeline models in the context of a hydraulic PTO for wave-energy harvesting. Several design cases are considered in which important parameters are varied, such as accumulator capacitance and pipeline length. This section describes the system, design cases, and pipeline models considered. Then the section specifies the variables considered to be appropriate

metrics for hydraulic PTOs in wave energy systems and by which the performance of the pipeline models are compared.

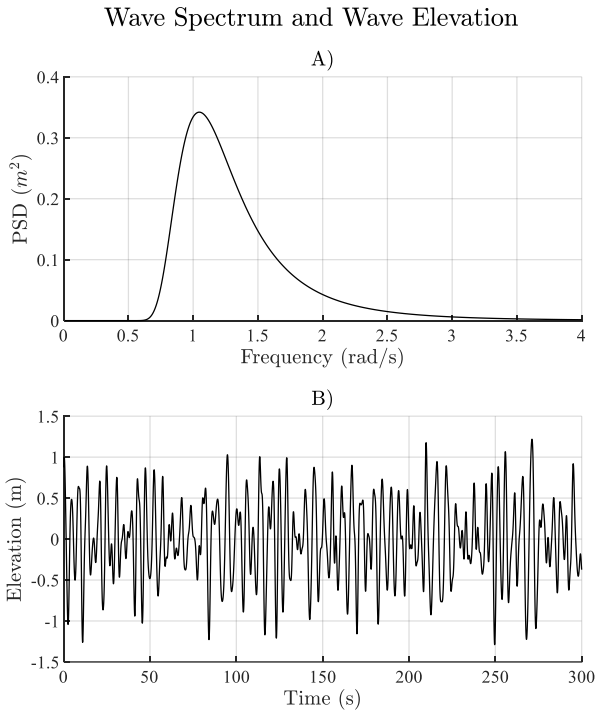

FIGURE 2. EXAMPLE POWER SPECTRAL DENSITY AND SIMULATED WAVE ELEVATION FOR A FIXED LOCATION IN TIME

The System

The PTO system considered has the WEC driving a pump offshore and the load on the system (e.g. a RO module) located onshore. The PTO's hydraulic circuit is shown in Figure 3. This circuit includes 1) a pump (e.g. a linear pump driven by a buoy or a rotary pump driven at the axis of a flap-type WEC, 2) low and high-pressure pipelines, 3) a load resistance, 4) a low-pressure accumulator (LHA) at inlet of the pump, 5) a high-pressure accumulator (HPA) at the outlet of the pump, and 6) a HPA at the high-pressure node of the load resistance. The low-pressure node of the load resistance has a fixed pressure that replicates the case that a kinetic charge pump is acting to maintain a fixed, elevated pressure in the low-pressure branch of the circuit.

Design Cases

The parameters specified for the design cases are given in Table 1 and are described as follows:

- **A** through **D** – Four cases with increasing capacitance (as if increasing accumulator volume) with the HPAs offshore and onshore having equal capacitance and pipelines having a length about 25 percent of the peak input wavelength (i.e. 1000 meters).
- **E** and **F** – Two cases identical to case B but with the total HPA capacitance unevenly distributed between offshore and onshore.
- **G** though **I** – Three cases identical to cases B, E, and F, respectively, but with shorter pipelines which have a length about 2 percent of the peak input wavelength (i.e. 100 meters).
- **J** – One case identical to case B where the entrained air content is elevated.
- **K** – One case where the length of the pipeline is approximately half the length of the peak input wavelength (i.e. 2200 meters), in which case the line frequency is equal to the peak input frequency.

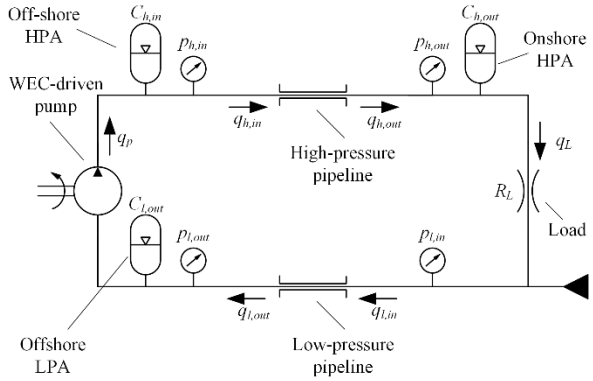

FIGURE 3. SCHEMATIC OF THE PTO HYDRAULIC CIRCUIT WITH MODELING VARIABLES

For all design cases, the peak wave period is 6 second, the load resistance and pump flow parameter X_p are set to give a nominal pressure in the high-pressure branch of 6 MPa with a 100-kW average load power. (Details about X_p are given in the following section). The fixed pressure at the low-pressure side of the load is varied based on the capacitance of the LPA so that the pressure at the inlet of the pump does not fall below 0.5 MPa. Finally, as a reference, the capacitance values given in Table 1 are translated to equivalent initial charge volumes for isothermally expanding, ideal gas under conditions specified in the table.

Pipeline Models

The five pipeline models tested are:

1. **Short line model** – only the flow resistance of the pipeline is modeled.
2. **Medium line model** – a single nominal Pi lump is used to model the flow resistance, capacitance, and inertia of the fluid in the pipeline.
3. **N π-lumps model** – a network of N nominal π-lumps are used to approximate the distributed nature of the flow resistance, capacitance, and inertia of the fluid in the pipeline. The value N is chosen to give segment

lengths as close to but less than 4 percent of the peak input wave length.

4. **Method of characteristics with constant properties and fixed grid (fMOC)** – the method of characteristics is used to obtain an explicit solution to the pressure and flow in a fixed, staggered grid.
5. **Discrete free-gas model using Method of Characteristics (DGCM)** – the fMOC is augmented with discrete gas volumes at nodes in a fixed staggered grid to capture the effects of entrained air in the working fluid on the wave speed.

Metrics

The metrics that will be compared between pipeline models are:

- The average power loss in each pipeline
- The standard deviation of the pressure in each accumulator
- The peak rate of change in pressure in the onshore HPA. The 99.7-percentile value will be used due to the stochastic nature of the problem
- The mean and standard deviation of the pressure differential across the WEC-driven pump

These choices give an account of the variables that a system designer would be concerned about in the analysis of a hydraulic WEC PTO. The rate of change in pressure is specific to the design of wave-powered RO systems where manufactures have placed constraints on the rate of change in pressure in the RO module. We ignore mean pressure in the accumulators because the differences are insignificant. However, wave delay effects could affect the mean pressure differential across the WEC-driven pump, and therefore it is reported to test this notion.

MODELING

The following mathematical models were used to simulate the plant shown in Figure 3. The nomenclature follows from that schematic. This section reports the simple elements of the system first. This is followed by a model of the pump flow generated by the WEC motion in irregular waves and, then descriptions of the pipeline models. The section concluded with details about implementation of the model.

System Model

The pressure nodes are governed by the capacitance of the accumulators such that

$$C_i \frac{dp_i}{dt} = q_{in} - q_{out} \tag{2}$$

where C_i is the capacitance located at node i and the subscripts "in" and "out" refer to the inflow and out flow of node i, generally. The flow rate through the load is governed by the resistance such that

$$R_L q_{load} = p_{h,out} - p_{l,in} \tag{3}.$$

Pump Flow

To replicate the flow from a WEC-driven pump, the pump flow is constructed from an inverse Fourier transformation of a typical power spectral density (PSD) for wave elevations like

TABLE 1. DESIGN CASE PARAMETERS

	Design Cases										
	A	B	C	D	E	F	G	H	I	J	K
Working Fluid: Water											
Density (kg/m^3)	1023										
Viscosity (Pa.s)	$9.4\text{x}10^{-4}$										
Bulk modulus (GPa)	2.2										
Air volume fraction at 101.3 kPa	0.0001									0.001	0.0001
Pump Flow											
X_q (m^3)	0.103										
Peak wave period, T_p (s)	6										
Load											
Resistance (Pa.s/m^3)	$2.83\text{x}10^8$										
Tank Pressure (MPa)	1.8	1.35	1.1	0.95	1.35						
Low-pressure high-pressure pipelines											
Length (m)	1000						100			1000	2200
Diameter (m)	0.15						0.1			0.15	
Offshore low-pressure accumulator											
Capacitance (m^3/Pa)	$1\text{x}10^{-7}$	$2\text{x}10^{-7}$	$4\text{x}10^{-7}$	$8\text{x}10^{-7}$	$2\text{x}10^{-7}$						
Charge volume equivalent at 0.5 MPa with charge pressure at 0.15 MPa (L)	167	333	667	1333	333						
Offshore high-pressure accumulator											
Capacitance (m^3/Pa)	$5\text{x}10^{-8}$	$1\text{x}10^{-7}$	$2\text{x}10^{-7}$	$4\text{x}10^{-7}$	$1\text{x}10^{-8}$	$1.9\text{x}10^{-7}$	$1\text{x}10^{-7}$	$1\text{x}10^{-8}$	$1.9\text{x}10^{-7}$	$1\text{ x}10^{-7}$	
Charge volume equivalent at 6 MPa with 4 MPa charge pressure (L)	450	900	1800	3600	90	1710	900	90	1710	900	
Onshore high-pressure accumulator											
Capacitance (m^3/Pa)	$5\text{x}10^{-8}$	$1\text{x}10^{-7}$	$2\text{x}10^{-7}$	$4\text{x}10^{-7}$	$1.9\text{x}10^{-7}$	$1\text{x}10^{-8}$	$1\text{x}10^{-7}$	$1.9\text{x}10^{-7}$	$1\text{x}10^{-8}$	$1\text{ x}10^{-7}$	
Charge volume equivalent at 6 MPa with 4 MPa charge pressure (L)	450	900	1800	3600	1710	90	900	1710	90	900	

that shown in Figure 2. This transformation is used to generate a predetermined pump flow as a function of time. This method neglects the effects of the system pressures variation on the WEC load; however, the purpose of this simplified approach, rather than simulating a WEC in the time domain, is to keep the inputs to the PTO the same between models.

To simplify generation and scaling of an input to the PTO model, the concept of a response amplitude operator (RAO) is used. The RAO, given as $\mathcal{R}(\omega)$, is a transfer function relating the amplitude of motion of a wave excited body to the amplitude of the wave elevation, where ω is the wave frequency. This is defined by

$$S_R(\omega) = \mathcal{R}(\omega)^2 S_w(\omega) \tag{4}$$

where S_w is the wave elevation PSD and S_R is the PSD for the WEC position. A commonly used PSD for fully developed sea conditions is the Pierson-Moskowitz spectrum [29], given by

$$S_w(\omega) = 5\pi^4 \frac{H_s^2}{T_p^4} \frac{1}{\omega^5} exp\left(\frac{-20\pi^4}{T_p^4 \omega^4}\right) \tag{5}$$

where H_s is the significant wave height and T_p is the peak wave period.

A pump flow can be found as follows. With the motion of the WEC coupled the pump, the velocity of the pump is found from the derivative of the WEC position such that

$$\dot{\Theta}(\omega) = j\omega\Theta(\omega) = j\omega S_R(\omega) \tag{6}.$$

Considering that the pump flow is proportional to the pump velocity,

$$Q_p(\omega) = D\dot{\Theta}(\omega) \tag{7}$$

where D is the pump displacement. Then, defining a wave elevation PSD normalized to the significant wave height,

$$\hat{S}(\omega) = \frac{S_w(\omega)}{H_s^2} \tag{8},$$

and defining a pump flow magnitude parameter,

$$X_q(\omega) = D\mathcal{R}(\omega) H_s \sqrt{2} \tag{9},$$

provides the following expression for pump flow in the time domain, where the PSD for the pump flow is transformed to the time domain using a summation of sinusoids.

$$q_p(t) = \left| \sum_{i=1}^{n} \left(X_q(\omega_i) \sqrt{{\omega_i}^2 \hat{S}(\omega_i) \Delta\omega} \right) \sin(\omega_i t + \varphi_i) \right| \tag{10}$$

The phase of each frequency component, φ_i, is random and distributed uniformly between $-\pi$ and π. The bin sizing of the PSD for each frequency component is $\Delta\omega$ and is constant.
While $\mathcal{R}(\omega)$ represents the dynamic response for specific WEC designs, and therefore, $X_q(\omega)$ would generally be a function of wave frequency, only constant values for X_q are considered in this work. Therefore, the frequency content of the input to the PTO is only a function of the wave elevation PDF and may be more or less widely distributed than is realistic.

Pipeline Models

The lumped parameter models are composed of lumped resistive, capacitive, and inertive elements. Using the Darcy-Weisbach equation, the pressure differential of the resistance elements is

$$p_{in} - p_{out} = Rq \tag{11}$$

where R is the resistance parameter and is given by

$$R = fRe \frac{2\mu L}{\pi d^4} \tag{12}$$

where μ is the dynamic viscosity of the fluid, d is the internal diameter of the pipeline, L is the length of the pipeline, and the f is the friction factor. The friction factor is a function of the Reynolds number, Re, and is modeled for laminar and turbulent flow using the Blasius correlation for the turbulent regime and a linear interpolation in the transitional flow regime. This gives

$$f = \begin{cases} \frac{64}{Re} & if\ Re \le Re_1 \\ f(Re_1) + \frac{f(Re_2) - f(Re_1)}{Re_2 - Re_1}(Re - 2300) & if\ Re_1 < Re < Re_2 \\ 0.316 Re^{-\frac{1}{4}} & if\ Re \ge\ Re_2 \end{cases} \tag{13}$$

where the parameters Re_1 and Re_2 are bounds for the linearly interpolated transitional range for the Reynolds number. These are taken as 2300 and 4500, respectively.

The capacitive elements are governed by Eq. (2) with the capacitance parameter given by

$$C = \frac{V}{\beta_{eff}} \tag{14}$$

where V is the lumped volume and β_{eff} is the effective bulk modulus of the fluid mixture in that volume. The fluid volumes are modeled as isothermally compressed mixtures of the working fluid and entrained air. The gas is modeled as an ideal gas. This gives an effective bulk modulus that is a function of the operating pressure p, such that

$$\beta_{eff} = \frac{\beta}{1 + \beta \alpha_o p_o / p^2} \tag{15}$$

where β is the bulk modulus of the working fluid without entrained air and α_o is the entrained air volume fraction at the pressure p_o.

For inertial elements,

$$I\frac{dq}{dt} = (p_{in} - p_{out}) \tag{16}$$

where I is the inertance of the lumped fluid given by

$$I = \frac{\rho L}{AN} \tag{17}.$$

Here, ρ is the density of the fluid, L is the length of the pipeline, and A is the cross-sectional flow area of the pipeline.

The distributed parameter models are formulated using the method of characteristics with the assumption of a fixed wave speed and a negligible effect of the fluid velocity on the wave speed. The formulations are mathematically identical to the formulations given in [28], and will not be reproduced here for the sake brevity.

Model Implementation

The system is simulated using a variable time step, variable order, Runga-Kutta numerical solver intended for stiff systems. The solver used is built into MATLAB (i.e. the function "ode15s"). The relative and absolute error tolerances that parameterize the solver are chosen based on a convergence study of the metrics specified for this study using the medium line model.

The fMOC and DGCM models are solved on a fixed time step; therefore, the maximum step size for the variable time step solver was set to the smallest fixed time step used for the MOC solutions. Between the fixed time steps, the last solution from the pipeline model is used rather than extrapolations of the data from prior time steps.

The number of pipeline segments in the N π-lumps model were chosen to give pipeline segment lengths that are just less than 4 percent as long as the wavelength having twice the frequency of the peak wave frequency. The grid spacing for the MOC pipeline models were chosen based from a convergence study for the metrics specified for this study.

The simulation parameters are given in Table 2 and are case dependent, in general.

RESULTS

In this section, the results of each model are compared against the results of the DGCM. This model is assumed to be the more accurate model in the set as it offers the highest fidelity and is documented to give accurate results. Where error is reported, it is calculated as

$$Error = 100\%\frac{result - DGCM\ result}{DGCM\ result} \tag{18}.$$

TABLE 2. SIMULATION PARAMETERS BY DESIGN CASE

	Design case										
	A	B	C	D	E	F	G	H	I	J	K
Simulation											
Time span	1200										
Solver error tolerance, ode15s()											
Relative	1.00E-06										
Absolute											
Pump flow, inverse Fourier transformation											
Wave frequency range (rad/s)	[0.1, 10]										
Frequency bin size (rad/s)	0.005										
Random number generator seed (MATLAB function rng())	2										
Pipeline segments											
N π-lumps	6					3				6	13
fMOC	50					10	50	10		50	100
DGCM											

To demonstrate the behavior of these systems, the flow and pressure results for case B are plotted in Figure 4 and Figure 5, respectively. These results are obtained using the DGCM pipeline model. Data are shown for a 100 second portion of the total 1200 second simulation. The flow rates shown in Figure 4 include the flow rate for the WEC-driven pump and the load as well as flow rates at the inlet and outlet of each pipe.

The flow rates shown in Figure 4 show a considerable reduction in the variation of flow from between the pump and the load. However, the flow through the pipelines are still highly variable, with the flow through the low-pressure pipeline even reversing. At these flow rates, the Reynolds number is on the order of 100,000 and in the turbulent regime; combined with nonlinear resistance in the turbulent regime, this fluctuation would lead to an increase in the power loss in the pipeline. It is also interesting to point out that major variations in flow occur at very long time scales, about 10 to 20 seconds for the high-pressure pipeline and about 40 second for the low-pressure pipeline. The frequencies are about two orders of magnitude lower than the pipeline frequency and may be resonant frequencies of the system.

The pressures shown in Figure 5 are also highly variable, spanning a range of 3 MPa within the 100 period and show evidence of the inertive effects of the pipeline. The inertive effects are especially apparent in in the low-pressure pipeline where the outlet pressure clearly rises above the inlet pressure.

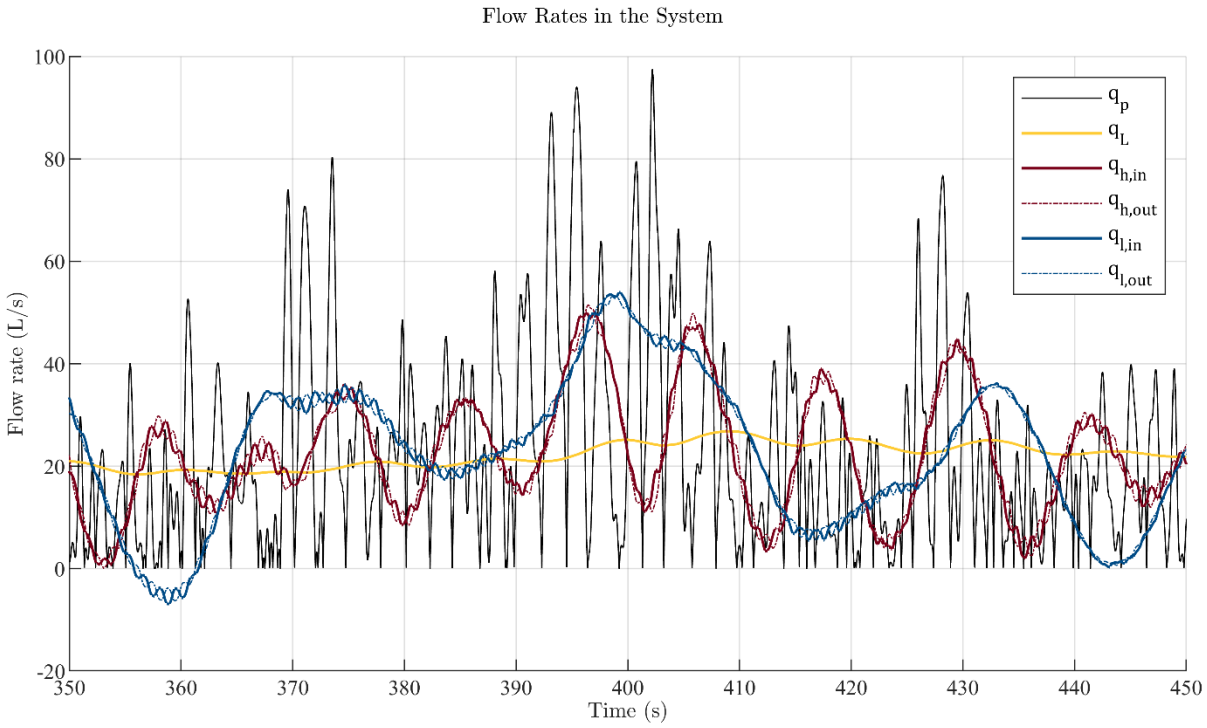

FIGURE 4. RESULTS FOR FLOW RATE WITHIN THE SYSTEM USING THE DGCM FOR DESIGN CASE B

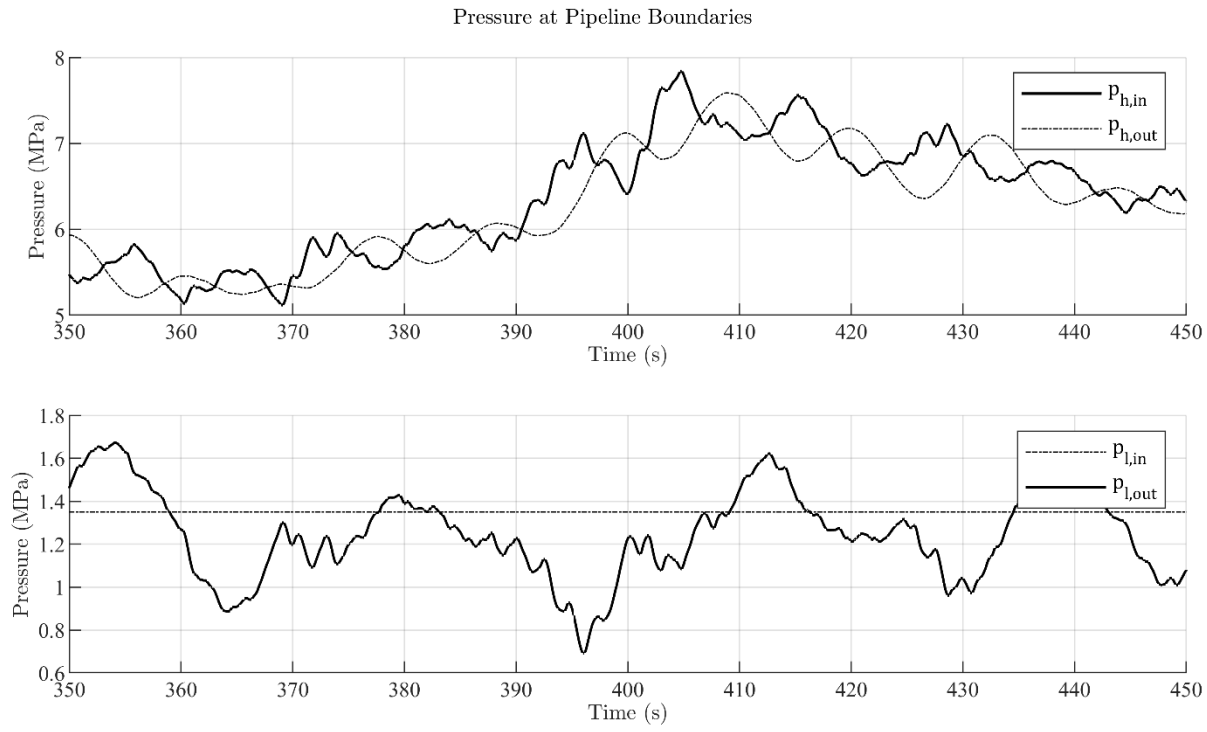

FIGURE 5. RESULTS FOR PRESSURE AT THE PIPELINE BOUNDARIES USING THE DGCM FOR DESIGN CASE B: (TOP) HIGH-PRESSURE PIPELINE AND (BOTTOM) LOW-PRESSURE PIPELINE

Results are also given for the distribution of pressure in Figure 6 over a period of two seconds. These results are for case K, where it is possible for a resonant condition to arise. These data show an instance where the pressure variation within the pipeline is greater than the pressure variation at the boundaries. This may have significant implications for the fatigue life of the pipeline if this is generally true.

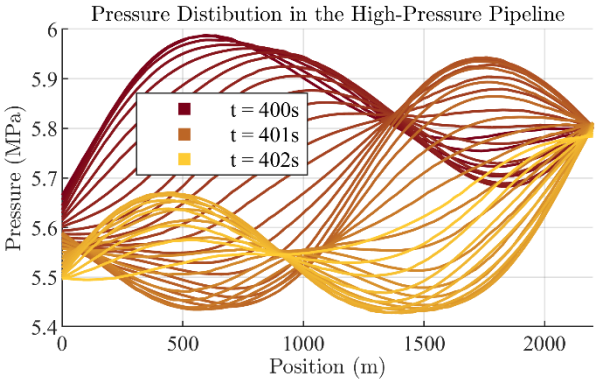

FIGURE 6. RESULTS FOR THE PRESSURE DISTRIBUTION ALONG THE HIGH-PRESSURE PIPELINE USING THE DGCM FOR DESIGN CASE K. DATA ARE PLOTTED OVER TWO SECONDS, BEGINING AT 400 SECONDS, AND IN INTERVALS OF 0.05 SECONDS.

The N π-lumps model gives results for pressure and flow within the pipe as well. These are compared to the DGCM for three instances during the same period for case K. There is some error, but the results match reasonably well as both models are capturing the same pressure waves in the pipeline.

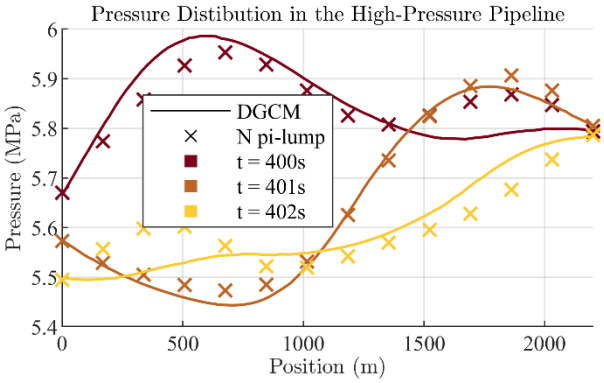

FIGURE 7. COMPARISON OF DGCM AND N PI-LUMP MODEL RESULTS FOR PRESSURE DISTRIBUTION ALONG THE HIGH-PRESSURE PIPELINE. RESULTS ARE FOR DESIGN CASE K.

Moving on to the design metrics, Figure 8 and Figure 9 give model results for the mean power loss in the low and high-pressure pipelines, respectively. Note that the sets of cases E, F and J and G, H, and I have identical parameters for the low-pressure pipeline, and therefore, only cases E and G are displayed from these sets in Figure 8. The error in results from the short line model are significant with up to a 22 percent underprediction for the power loss in the low-pressure pipeline and 74 percent underprediction for the high-pressure pipeline. All other models give good agreement with the DGCM. There is an exception with the high-pressure pipeline losses in design case E, where the capacitance at the pump outlet is lowest of all cases. In this case, the medium line model results overpredicts the losses by 13 percent. The N π-lumps model also gives higher error in design case E than in other cases but this is only about 1.9 percent error.

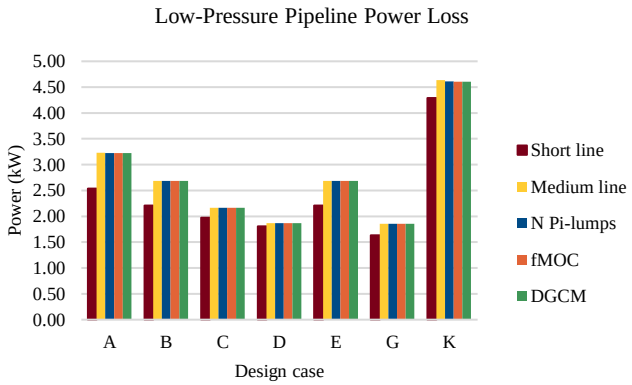

FIGURE 8. MODEL RESULTS FOR MEAN POWER LOSS IN THE LOW-PRESSURE PIPELINE BY DESIGN CASE

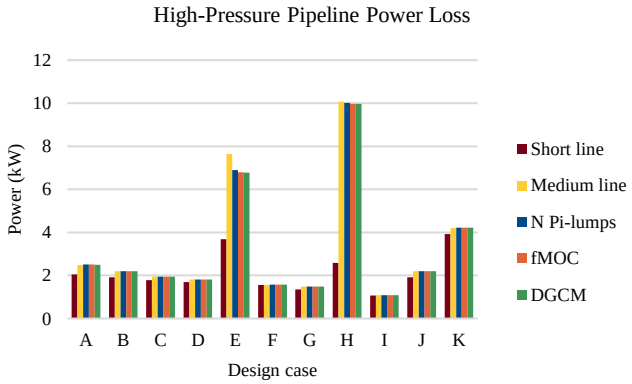

FIGURE 9. MODEL RESULTS FOR MEAN POWER LOSS IN THE HIGH-PRESSURE PIPELINE BY DESIGN CASE

The standard deviations in pressure at the three accumulators are given in Figure 10, Figure 11, and Figure 12. Again, parameters for the low-pressure branch of the circuit are repeated; repeated cases are left out of Figure 10. As with the power loss results, the performance of the short line model is poor in predicting the variation in pressure in the offshore LPA compared to all other models, with it underpredicting the variation by up to 77 percent compared the DGCM. The medium line model overpredicts the variation but only with it being up to 2.4 percent in error while the rest of the models are in good agreement with the DGCM with less than 1 percent error.

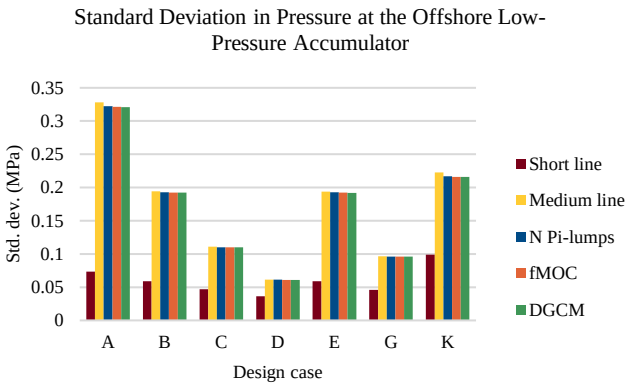

FIGURE 10. MODEL RESULTS FOR STANDARD DEVIATION IN PRESSURE IN THE OFFSHORE LPA

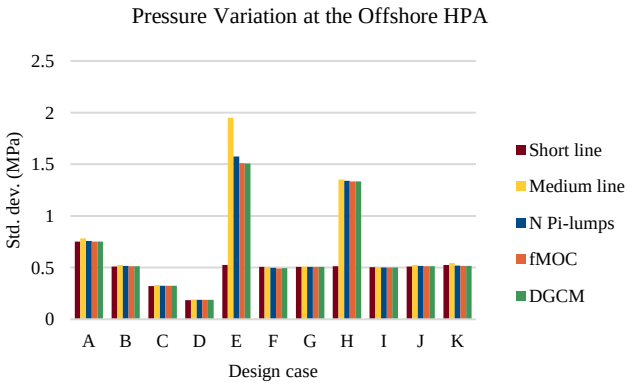

FIGURE 11. MODEL RESULTS FOR STANDARD DEVIATION IN PRESSURE IN THE OFFSHORE HPA

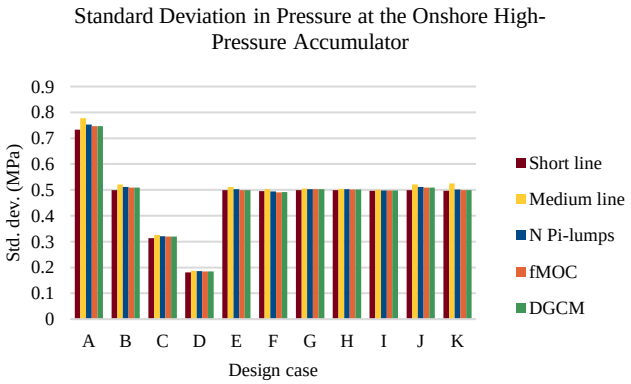

FIGURE 12. MODEL RESULTS FOR STANDARD DEVIATION IN PRESSURE IN THE ONSHORE HPA

The results for the standard deviation in the pressure in the HPAs is remarkably different than for the LPA. In many cases, the medium line and N π-lumps model perform worse than the short line model in predicting the variation in pressure. Notable exceptions are design cases E and H where the variation in the offshore HPA is underpredicted by the short line model by 65 percent and 61 percent, respectively. However, even in design case E, the medium line model and N π-lumps models give poorer results, overpredicting the variation by 29 and 4.4 percent error, respectively. The agreement of the models on the variation in pressure in the onshore HPA is relatively better than for the onshore HPA with a magnitude of error less than 3 percent from the short line model, less than 6 percent from the medium line model, and less that 1 percent error from the N π-lumps model. The medium line model constantly overpredicts the variation across design cases and is clearly the worst performer overall.

Figure 13 compares the results for the peak rate of pressure change at the onshore HPA. The short line gives poor agreement with the DGCM while the other models give more favorable results. The medium line model results are typically in the range of 1 to 4 percent error. The N π-lumps model gives less than 1 percent error in all cases except case B with 1.5 percent error and case F with -7 percent error.

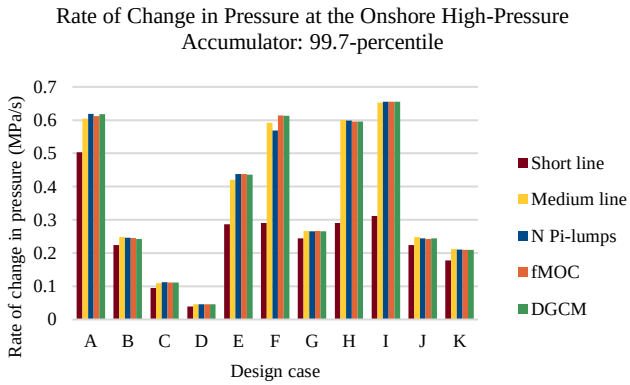

FIGURE 13. MODEL RESULTS FOR PEAK RATE OF CHANGE IN PRESSURE IN THE ONSHORE HPA (99.7-PERCENTILE)

Finally, Figure 14 and Figure 15 give results for the mean and standard deviation in the pressure differential across the WEC-driven pump, respectively. The agreement between models is very good in all cases with less than 0.2 percent error from the short line model and less than 0.05 percent error for all other models. The error for the variation in the pressure differential is relatively higher, as expected from previous results for pressure variation. Although, despite the very high error in the variation in the offshore LPA pressure shown in Figure 10, the magnitude of the error for all models, in all cases is less than 8 percent. The medium line model overpredicts by up to 5.1 percent while the magnitude of the N π-lumps model error is below 1 percent for all cases.

DISCUSSION

The results of this study suggest that the short line model is not sufficient for design analysis. The model gives results that are up 77 percent in error and the magnitude of error is

consistently an order of magnitude higher than the other lumped parameter models. In addition, metrics are consistently underpredicted, meaning the model would not be a conservative choice for design analysis.

The medium line model gives reasonably good agreement with the DGCM results with errors typically less that 5 percent in magnitude. However, it is susceptible to giving higher error in cases where the capacitance at the WEC-driven pump is low (e.g. design cases E and H). The N π-lumps model is less susceptible in these cases and give about 5 percent error in pressure variation. For this study, the number of segments were selected to give segment lengths less than or equal to 4 percent of the dominate wavelength. More segments would likely improve its performance; however, the 4 percent rule-of-thumb appears to be sufficient for most cases.

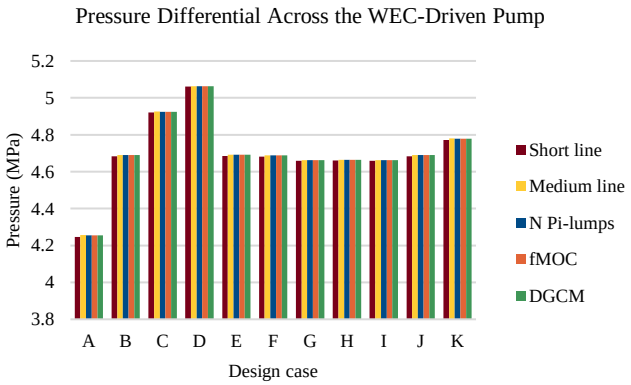

FIGURE 14. MODEL RESULTS FOR MEAN PRESSURE DIFFERENTIAL ACROSS THE WEC-DRIVEN PUMP

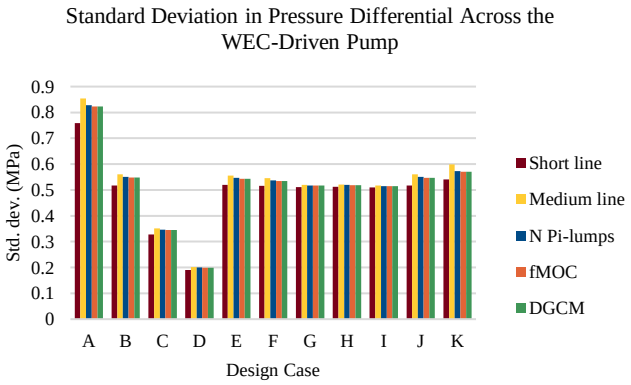

FIGURE 15. MODEL RESULTS FOR STANDARD DEVIATION IN THE WEC-DRIVEN PUMP PRESSURE DIFFERENTIAL

The results from the fMOC and DGCM are in very good agreement in all cases, suggesting that the pressure dependency of the bulk modulus for fluids having entrained air is not significant at the pressures considered for these simulations. The sensitivity of the bulk modulus to pressure when entrained air is present increases significantly at lower pressures but it is not reasonable to expect that these systems are intentionally designed to operate at such low pressures. Greater amounts of air entrainment would increase the range of pressures at which the bulk modulus is sensitive to pressure, but air entrainment for seawater is not expected to be any greater than the values tested. Therefore, the fMOC is expected to be adequate for analyses of stronger transients that require high accuracy. If very low pressures and cavitation are expected, then one should consider the DGCM.

It was noted that pressure variation within the pipeline seems to exceed the pressure variation at the boundaries. This is significant since fatigue analysis using pressure variations at the boundaries may overpredict the fatigue life of the pipeline. The N π-lumps, fMOC, and DGCM could be used to give more accurate accounts of stress fluctuation within the pipeline. N π-lumps was found to be in reasonable agreement with the DGCM for the pressure distribution within the pipeline and might be sufficient for this purpose; although it would be prudent to compare fatigue calculation between models to validate this claim.

The adequacy of the N π-lumps model for predicting the given design metrics is significant for wave energy developers for the simple fact that commercial software (e.g. MATLAB's Simscape Fluids) may only implement lumped parameter pipeline models. With the development of WEC-Sim by the National Renewable Energy Lab [30] being carried out in MATLAB and Simulink, system modelers and designers could readily use the Simscape Fluid's implementation of the N π-lumps model (called the "Segmented Pipeline" block in that case). In contrast, implementation of a distributed parameter model within the WEC-Sim framework would require some software development.

CONCLUSION

Several pipeline models were compared in the context of a generic wave-energy PTO with realistic wave inputs. The models were compared for several design cases that explored variations in parameters such as accumulator capacitance, pipeline length, and entrained air volume fraction. Variables that would be important to the system designer were compared, such as power loss, variation in pressure, and the rate of pressure change at the load (a variable specifically important to the application of wave-powered RO desalination). The results of this study suggest that for system designers interested in these metrics, the pipeline modeling guidelines found in literature can be slightly relaxed; that is, multi-segment lumped parameter models may replace distributed parameter models.

It is necessary to model the inertia of the pipeline, even for the relatively short 100-meter pipelines; otherwise, power losses and pressure variation may be underpredicted. The medium line model was still susceptible to error in design cases with low

capacitance at either end of the pipeline. In these cases, one can use multiple nominal π-lumps. A reasonable rule-of-thumb is to maintain a pipeline segment length that is less than or equal to 4 percent of the wavelength for the peak wave period.

The study performed does not consider all possible architectures for wave energy systems. For those that differ from the system considered in this work, designers are advised to consider distributed parameter models, especially for architectures that include strong disturbances to the pipeline at higher frequencies than typical ocean wave frequencies such as rapid switching of valves in a switch-mode circuit, as with the system considered in [31]. Further work considering systems with these types of disturbances may clarify the limits of pipeline models.

ACKNOWLEDGEMENT

This research was supported in part by an appointment with Marine and Hydrokinetic Graduate Student Research Program sponsored by the U.S. Department of Energy (DOE), Office of Energy Efficiency and Renewable Energy, and Water Power Technologies Office. This program is administered by the Oak Ridge Institute for Science and Education (ORISE) for the DOE. ORISE is managed by ORAU under DOE contract number DESC0014664.

All opinions expressed in this paper are the author's and do not necessarily reflect the policies and views of DOE, ORAU, or ORISE.

REFERENCES

[1] Gunn, K., and Stock-Williams, C., 2012, "Quantifying the Global Wave Power Resource," Renew. Energy, **44**, pp.296–304.

[2] Dudley, B., 2019, *BP Statistical Review of World Energy*.

[3] 2020, "International Energy Agency: Key World Energy Statistics."

[4] Fernández Prieto, L., Rodríguez Rodríguez, G., and Schallenberg Rodríguez, J., 2019, "Wave Energy to Power a Desalination Plant in the North of Gran Canaria Island: Wave Resource, Socioeconomic and Environmental Assessment," J. Environ. Manage., **231**, pp.546–551.

[5] Yu, Y.-H., and Jenne, D., 2017, "Analysis of a Wave-Powered, Reverse-Osmosis System and Its Economic Availability in the United States," *International Conference on Ocean, Offshore and Arctic Engineering*, Trondheim, Norway.

[6] Leijon, J., and Boström, C., 2018, "Freshwater Production from the Motion of Ocean Waves – A Review," Desalination, **435**(November 2017), pp.161–171.

[7] Folley, M., Suarez, B., and Whittaker, T., 2008, "An Autonomous Wave-Powered Desalination System," Desalination, **220**, pp.412–421.

[8] Yu, Y.-H., Tom, N., and Jenne, D., 2018, "Numerical Analysis on Hydraulic Power Take-Off for Wave Energy Converter and Power Smoothing Methods," *Proceedings of the ASME 2018 37th International Conference on Ocean, Offshore and Arctic Engineering*, Madrid, Spain.

[9] "Technology - Resolute Marine," accessed August 3, 2020, https://www.resolutemarine.com/technology/.

[10] Nolan, G., and Ringwood, J., 2006, "Control of a Heaving Buoy Wave Energy Converter for Potable Water Production," *Irish Signal and Systems Conference*, pp.421–426.

[11] Wilf, M., Awerbuch, L., Bartels, C., Mickley, M., Pearce, G., and Voutchkov, N., 2007, *The Guidebook to Membrane Desalination Technology: Reverse Osmosis, Nanofiltration and Hybrid Systems: Process, Design, and Applications and Economics*, Balaban Desalination, L'Aquila, Italy.

[12] Jane Kucera, 2015, *Reverse Osmosis*, John Wiley and Sons, Hoboken, New Jersey.

[13] 2020, *FilmTec™ Reverse Osmosis Membranes*, DuPont, Form No. 45-D01504-en, Rev. 3.

[14] Wang, K., Abdalla, A. A., Khaleel, M. A., Hilal, N., and Khraisheh, M. K., 2017, "Mechanical Properties of Water Desalination and Wastewater Treatment Membranes," Desalination, **401**, pp.190–205.

[15] Hicks, D. C., Please, C. M., Mitcheson, G. R., and Salevan, J. F., 1989, "Delbuoy: Ocean Wave-Powered Seawater Reverse Osmosis Deslination System," Desalination, **73**, pp.81–94.

[16] Whittaker, T., and Folley, M., 2012, "Nearshore Oscillating Wave Surge Converters and the Development of Oyster," Philos. Trans. R. Soc. A Math. Phys. Eng. Sci., **370**, pp.345–364.

[17] Grainger, J. J., and Stevenson, W. D., 1994, *Power System Analysis*, McGraw-Hill.

[18] Watton, J., 2009, *Fundamentals of Fluid Power Control*, Cambridge University Press.

[19] Ghidaoui, M., Zhao, M., Mcinnis, D. A., and Axworthy, D. H., 2005, "A Review of Water Hammer Theory and Practice," Appl. Mech. Rev., **58**(January), pp.49–76.

[20] Watton, J., and Tadmori, M. J., 1988, "A Comparison of Techniques for the Analysis of Transmission Line Dynamics in Electrohydraulic Control Systems," Appl. Math. Model., **12**(5), pp.457–466.

[21] Soumelidis, M. I., Johnston, D. N. N., Edge, K. A., and Tilley, D. G., 2005, "A Comparative Study of Modelling Techniques for Laminar Flow Transients in Hydraulic Pipelines," Proc. JFPS Int. Symp. Fluid Power, **2005**(6), pp.100–105.

[22] Leon, A., Ghidaoui, M. S., Schmidt, A. R., and Garcia, M. H., 2007, "An Efficient Finite-Volume Scheme for Modeling Water Hammer Flows," J. Water Manag. Model., (January).

[23] Zhou, L., Li, Y., Zhao, Y., Ou, C., and Zhao, Y., 2021, "An Accurate and Efficient Scheme Involving Unsteady Friction for Transient Pipe Flow," J. Hydroinformatics, **23**(4), pp.879–896.

[24] Krus, P., Weddfelt, K., and Palmberg, J. O., 1994, “Fast Pipeline Models for Simulation of Hydraulic Systems,” J. Dyn. Syst. Meas. Control. Trans. ASME, **116**(1), pp.132–136.
[25] Johnston, N., 2012, “The Transmission Line Method for Modelling Laminar Flow of Liquid in Pipelines,” Proc. Inst. Mech. Eng. Part I J. Syst. Control Eng., **226**(5), pp.586–597.
[26] Wylie, E. B., 1965, “Pressure Transients in Viscous Fluid Systems,” J. Basic Eng., **87**(4), pp.1089–1089.
[27] Yudell, A. C., and Van de Ven, J. D., 2017, “Experimental Validation of a Time Domain Cavitation Model for Switched Inertance Circuits,” *Proceedings of the ASME/BATH Symposium on Fluid Power and Motion Control*, Sarasota, FL.
[28] Wylie, E. B., Streeter, V. L., and Suo, L., 1993, *Fluid Transients in Systems*, Prentice-Hall.
[29] Pierson, W. J., and Moskowitz, L., 1964, “A Proposed Spectral Form for Fully Developed Wind Seas Based on the Similarity Theory of S. A. Kitaigorodskii,” J. Geophys. Res., **69**(24), pp.5181–5190.
[30] Yu, Y.-H., Lawson, M., Ruehl, K., and Michelen, C., 2014, “Development and Demonstration of the WEC-Sim Wave Energy Converter Simulation Tool,” 2nd Mar. Energy Technol. Symp., pp.1–8.
[31] Simmons II, J. W., and Van de Ven, J. D., 2019, “Switch-Mode Power Transformer in a Wave-Powered, Reverse Osmosis Desalination Plant,” *ASME/BATH 2019 Symposium on Fluid Power and Motion Control*, ASME, Sarasota, FL.